

Cardiac Adrenergic Innervation Is Affected in Asymptomatic Subjects with Very Early Stage of Coronary Artery Disease

Sakari Simula, MD¹; Esko Vanninen, MD, PhD²; Laura Viitanen, MD¹; Anu Kareinen, MD¹; Seppo Lehto, MD, PhD¹; Pia Pajunen, MD³; Mikko Syväne, MD, PhD³; Jyrki Kuikka, PhD²; Markku Laakso, MD, PhD¹; and Juha Hartikainen, MD, PhD¹

¹Department of Medicine, Kuopio University Hospital, Kuopio, Finland; ²Department of Clinical Physiology and Nuclear Medicine, Kuopio University Hospital, Kuopio, Finland; and ³Department of Medicine, Division of Cardiology, Helsinki University Central Hospital, Helsinki, Finland

The aim of this study was to investigate whether, in subjects with a very early stage of coronary artery disease without hemodynamically significant coronary artery stenoses, cardiac adrenergic innervation is already affected. **Methods:** Quantitative coronary angiography and dual-isotope SPECT with ¹²³I-metaiodobenzylguanidine (MIBG) and ^{99m}Tc-sestamibi (MIBI) were conducted to assess the function of cardiac adrenergic innervation and myocardial perfusion, respectively, in 30 asymptomatic volunteers with a high familial risk for coronary artery disease. Regional quantitative analysis of MIBG uptake and washout rates was performed using the SPECT data from the anteroseptal, lateral, and inferior myocardial regions, which represented vascular supply by the left anterior descending coronary artery (LAD), left circumflex coronary artery (LCX), and right coronary artery (RCA), respectively. **Results:** The average severity of stenoses was 33% ± 11% in the LAD, 29% ± 14% in the LCX, and 26% ± 19% in the RCA. The severity of stenosis was not related to MIBI uptake in any corresponding myocardial region at rest or during exercise. However, the degree of LAD stenosis correlated directly with delayed MIBG uptake ($r = 0.43$; $P < 0.05$) and inversely with MIBG washout ($r = -0.34$; $P = 0.06$) of the anteroseptal myocardium. When subjects were divided into tertiles according to the separate severity of stenosis for each coronary artery, delayed MIBG uptake in the anteroseptal region was significantly lower in the lowest LAD tertile (0.34 ± 0.05) than in the middle (0.41 ± 0.06 ; $P < 0.01$) or highest (0.43 ± 0.05 ; $P < 0.001$) LAD tertile. Correspondingly, delayed MIBG uptake in the lateral region was also lower in the lowest LCX tertile than in the middle tertile (0.34 ± 0.04 vs. 0.41 ± 0.06 , respectively; $P < 0.01$). Washout rate was also higher in the lowest LAD tertile ($44\% \pm 7\%$) than in the middle ($36\% \pm 10\%$; $P < 0.05$) or highest LAD tertile ($34\% \pm 8\%$; $P < 0.01$). **Conclusion:** The degree of coronary artery stenosis was associated directly with MIBG uptake and inversely with MIBG washout. This finding suggests that the function of cardiac

adrenergic nerve endings is modified even in mild coronary artery disease before denervation occurs.

Key Words: ¹²³I-metaiodobenzylguanidine; cardiac adrenergic function; coronary artery disease

J Nucl Med 2002; 43:1-7

Coronary artery disease is a slow process, taking several years before hemodynamically significant stenoses develop. On the other hand, evidence shows that the endothelial regulation of coronary artery flow becomes impaired during the very early stage of coronary atherosclerosis and even in patients with hypercholesterolemia (1-4). Endothelial dysfunction results in paradoxical vasoconstriction of coronary arteries in response to adrenergic activation and predisposes to impaired coronary perfusion and myocardial ischemia (5). Moreover, progression of atherosclerotic disease has been shown to be associated with progressive impairment of endothelial function (2,6,7).

Myocardial infarction results in cardiac adrenergic denervation (8-11). In addition, dysfunction of adrenergic nerve endings has been reported in patients with severe coronary artery disease without myocardial infarction (12,13). During myocardial ischemia, noradrenaline spillover increases, and it has been suggested that this reflects increased adrenergic tone (14,15). However, the net transportation direction of catecholamines is reversed; that is, as the first step in acute ischemia, washout decreases because of lactate production (16). This reversal has also been shown in pacing-induced ischemia, in which net cardiac noradrenaline release, present before ischemia, reverts to net uptake during ischemia (17). Thus, a challenging question is whether the function of adrenergic nerve endings is modified similarly to endothelial function during the early phase of coronary atherosclerosis before hemodynamically significant stenoses and adrenergic denervation occur.

Received Sep. 13, 2000; revision accepted Jan. 17, 2001.

For correspondence or reprints contact: Juha Hartikainen, MD, PhD, Department of Medicine, Kuopio University Hospital, P.O. Box 1777, 70211 Kuopio, Finland.

E-mail: juha.hartikainen@kuh.fi

The function of cardiac adrenergic innervation can be assessed noninvasively with ^{123}I -metaiodobenzylguanidine (MIBG), a noradrenaline analog taken up into the nerve endings by a specific, energy-dependent uptake-1 mechanism (18). Recently, new techniques, such as measurement of MIBG washout, have enabled more detailed assessment of the function and integrity of adrenergic innervation.

In this study, we performed quantitative coronary angiography and dual-isotope scintigraphy imaging with MIBG and $^{99\text{m}}\text{Tc}$ -sestamibi (MIBI) to study cardiac adrenergic innervation and myocardial perfusion, respectively, in subjects free of any anginal symptoms but with a high familial risk for coronary artery disease. Specifically, we evaluated whether myocardial MIBG kinetics, reflecting cardiac adrenergic function, are affected during the early phase of coronary artery disease.

MATERIALS AND METHODS

Subjects

The study population consisted of 30 subjects free of angina pectoris (18 men, 12 women; age range, 43–68 y; mean age, 55 ± 7 y) from families with early-onset coronary artery disease. The family history was considered positive if at least 2 siblings of the subject had severe coronary artery disease, that is, angiographically diagnosed 3-vessel disease with a 50% cutoff or myocardial infarction occurring at a young age (<55 y). In other words, all recruited subjects were asymptomatic siblings of patients with symptomatic coronary artery disease. Subjects with diseases known to influence the autonomic nervous system, such as diabetes mellitus, Parkinson's disease, or atrial fibrillation, were excluded.

For at least 12 h before MIBG imaging, the subjects were not allowed to drink coffee, tea, or cola beverages or to smoke. In addition, all medical therapy known to influence MIBG uptake was discontinued before the study (19).

Protocol

The study protocol consisted of quantitative coronary angiography, radionuclide studies at rest, and radionuclide studies during maximal bicycle exercise testing. The subjects gave written informed consent after the nature and possible risks associated with investigations were explained to them in detail. The study protocol was approved by the local ethics committee.

Angiographic Analyses

Coronary angiography was performed by the percutaneous femoral approach using standard angiographic techniques. Four views of the left and right coronary arteries were recorded on cine film. Intracoronary nitroglycerin (250 μg) was administered before the angiographic imaging was performed.

Quantitative analysis of coronary angiography data was performed with a previously validated method (Cardiovascular Measurement System; Medis, Neunen, The Netherlands) (20,21). The optimal frame—with full opacification of the vessel, minimal motion blurring, and minimal overlapping with other branches—was selected and was usually at end-diastole or during diastasis. The frames were selected by a cardiologist experienced in quantitative analysis of coronary angiograms. Vessel edges were mea-

sured with a computerized edge-detection algorithm. Luminal diameters were measured using the dye-filled guiding catheter as a reference, and severity of stenoses (percentage of lumen diameter) was calculated. All stages of the angiographic analyses were performed without knowledge of the patients' clinical characteristics.

Exercise Test

A maximal symptom-limited exercise test was performed with a bicycle ergometer during temporary withdrawal of β -blocking and calcium channel-blocking agents. A protocol of 20 W initial workload and increments of 20 W/min was used. The test was terminated if any of the following criteria were met: severe angina pectoris, exhaustion, or decrease in systolic pressure ≥ 10 mm Hg during exercise. Myocardial ischemia was defined as horizontal or downsloping ST depression ≥ 0.1 mV measured at J point + 60 ms. In addition, maximal oxygen uptake was calculated.

Radionuclide Studies

Cardiac SPECT was performed using MIBG (MAP Medical Technologies Oy, Helsinki, Finland) to assess cardiac adrenergic innervation. Myocardial perfusion was evaluated using MIBI (DuPont Pharmaceuticals, Hertfordshire, U.K.) at rest and during exercise on 2 consecutive days. MIBG imaging and MIBI imaging at rest were performed during the first day. Myocardial perfusion during exercise was assessed on the following day. The specific activity of MIBG was 26,000 MBq/mmol. During the first day, 400 MBq MIBI tracer, followed by 200 MBq MIBG tracer 15 min later, were injected into the left antecubital vein. The first SPECT scan was started 30 min after MIBI injection to study myocardial perfusion and initial MIBG uptake. The second SPECT scan was obtained 4 h and 5 min after MIBG injection using the same imaging settings to study late MIBG uptake. On the next day, to assess perfusion during exercise, a dose of 400 MBq MIBI tracer was injected during the last minute of maximal stress and imaging was started 30 min after the injection. In addition, to assess global myocardial MIBG and MIBI uptake, the first planar scan was started 25 min after the MIBI injection and the second was obtained 4 h after injection.

A Multispect 3 gamma camera (Siemens Gammasonics, Des Plaines, IL) equipped with high-resolution collimators was used to assess myocardial distribution of MIBG and MIBI tracers. The imaging resolution was 13–14 mm. Three detectors ($3 \times 120^\circ$) acquired 30 views with 4° steps of 45 s each. The matrix size was 128×128 without zooming, and the voxel size was $3 \times 3 \times 3$ mm. The energy window of $^{99\text{m}}\text{Tc}$ was centered at $140 \text{ keV} \pm 6\%$, and that of ^{123}I was shifted to $158 \text{ keV} \pm 5.5\%$. Overlapping of the energies was corrected using a matrix inversion technique with the standard doses of ^{123}I and $^{99\text{m}}\text{Tc}$. Overlapping of ^{123}I activity onto the $^{99\text{m}}\text{Tc}$ window was, on average, 18%; vice versa, the overlap was 4%.

Data Analysis

The raw data of MIBG and MIBI SPECT studies were reconstructed using a Butterworth-filtered (order, 8; cutoff frequency, 0.65 cm^{-1}) backprojection technique. For semiquantitative analysis of regional uptake on both initial and delayed images, interpolative background subtraction was used to reduce the effect of background activity. Transaxial slices were reconstructed and reoriented to represent coronal slices. Using a semiautomatic quantification program (Quantitative Heart Application; Siemens

Gammasonics), mean counts were recorded from anterior, lateral, inferior, and septal regions.

Mean myocardial MIBG and MIBI counts obtained from initial and delayed planar imaging were normalized by the mean upper-mediastinal counts of the respective images and expressed as heart-to-mediastinum ratio (H/M). For assessment of regional uptake of the MIBG and MIBI tracers, the myocardium was divided into 8 segments (Fig. 1). MIBG and MIBI uptake was measured from the following coronary artery territories as previously described (22). The left anterior descending coronary artery (LAD) region included the anterior and septal areas (segments 1–4), the left circumflex coronary artery (LCX) region included the lateral area (segments 5–6), and the right coronary artery (RCA) region included the inferior area (segments 7–8) of the myocardium. Regional MIBG and MIBI uptake was normalized to the maximal myocardial uptake of the tracer and expressed as normalized units. The apex and the most basal layer were excluded from the analysis. The rater was unaware of the clinical data and angiographic findings.

Regional quantitative analysis of MIBG washout rate was calculated using the initial and delayed images. The regional washout rate was calculated as follows: $(A - B)/A \times 100$, where A is the mean counts for the region of interest on the initial image and B is mean counts on the delayed image.

Statistical Methods

To estimate the significance of differences between groups, 1-way ANOVA was performed. When differences were found, the Tukey test was used as a posthoc analysis for continuous variables. In addition, the χ^2 test was used for categoric variables when appropriate. A least squares regression analysis was used to study univariate linear correlations. $P < 0.05$ was considered statistically significant. Results are expressed as mean \pm SD.

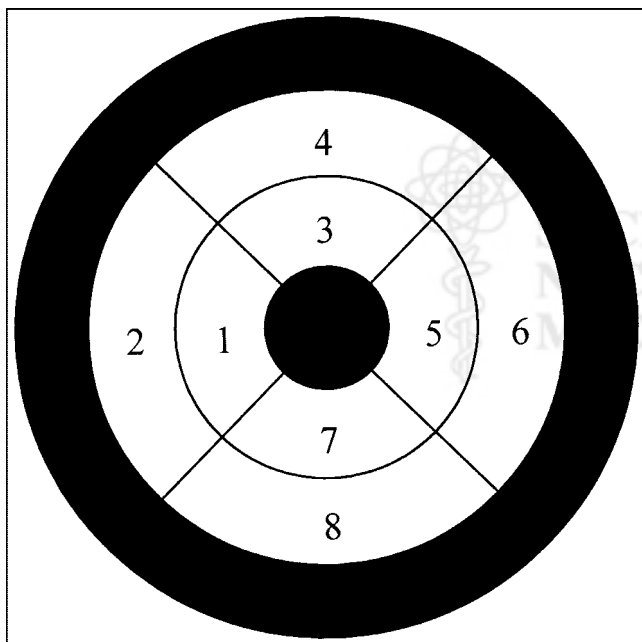


FIGURE 1. Schematic representation of myocardium divided into 8 segments. Segments 1–4 represent anteroseptal, 5–6 lateral, and 7–8 inferior myocardium. Black areas indicate myocardial regions excluded from analysis (apex in center and most basal layer on border).

TABLE 1
Clinical Characteristics of Subjects

Characteristic	Value
Female/male	12/18
Age (y)	55 \pm 7 (43–68)
BMI (kg/m ²)	28 \pm 3 (21–36)
Hypertension	11 (37%)
Smokers (active or previous)	11 (37%)
fB-gluc (mmol/L)	5.6 \pm 0.6 (4.8–6.5)
Lipid profile	
Total cholesterol (mmol/L)	6.9 \pm 1.1 (4.0–8.7)
HDL cholesterol (mmol/L)	1.3 \pm 0.3 (0.8–1.7)
LDL cholesterol (mmol/L)	4.8 \pm 1.0 (2.2–6.5)
Triglycerides (mmol/L)	1.9 \pm 1.2 (0.9–3.2)
Medication	
β -blocking agents	4 (13%)
Calcium channel-blocking agents	3 (10%)
ACE inhibitors	5 (10%)
Lipid-lowering drugs	4 (13%)

BMI = body mass index; fB-gluc = fasting blood glucose; HDL = high-density lipoprotein; LDL = low-density lipoprotein; ACE = angiotensin-converting enzyme.
Values are mean \pm SD and range or *n* (%).

RESULTS

The subjects had no evidence of typical angina pectoris or dyspnea in their medical history, but 11 (37%) were hypertensive and 5 (17%) were smokers at the time of the study. The clinical characteristics of the subjects are shown in Table 1. None had anginal symptoms during exercise testing, but 13 (43%) presented with ST depression. For all subjects, the reason for termination of exercise was exhaustion. The results of exercise testing are shown in Table 2.

Quantitative Coronary Angiography

The results of quantitative coronary angiography are shown in Table 3. The severity of stenosis averaged 33% \pm 11% (range, 0%–54%) in the LAD, 29% \pm 14% (range,

TABLE 2
Results of Exercise Test

Parameter	Value
DAP at rest (mm Hg)	82 \pm 11
SAP at rest (mm Hg)	140 \pm 18
HR at rest (bpm)	77 \pm 14
SAP max during exercise (mm Hg)	221 \pm 22
HR max during exercise (bpm)	168 \pm 13
VO ₂ max during exercise (mL/kg/min)	31 \pm 7
Max workload (W)	189 \pm 46
ST depression \geq 0.1 mV	13 (43%)
Workload at ST depression (W)	155 \pm 42

DAP = diastolic arterial pressure; SAP = systolic arterial pressure; HR = heart rate; max = maximal value; VO₂ = estimated oxygen uptake.
Values are mean \pm SD or *n* (%).

TABLE 3
Angiographic Severity of Coronary Artery Stenoses

Subject no.	LM (%)	LAD (%)	LCX (%)	RCA (%)
1	0	38	38	36
2	0	45	29	30
3	0	17	39	0
4	0	26	0	0
5	24	44	31	73
6	18	54	27	42
7	0	33	38	51
8	0	27	27	27
9	0	39	31	12
10	0	0	34	2
11	0	31	29	21
12	0	28	37	24
13	0	31	43	27
14	0	46	24	37
15	0	16	18	0
16	0	33	24	23
17	0	29	12	39
18	0	38	17	13
19	0	22	20	32
20	29	36	39	50
21	0	51	36	0
22	0	39	70	46
23	0	33	31	29
24	0	26	20	22
25	0	37	31	30
26	0	32	44	46
27	0	32	0	0
28	0	29	34	38
29	0	29	29	30
30	0	35	0	0
Mean \pm SD	3 \pm 8	33 \pm 11	29 \pm 14	26 \pm 19

LM = left main.

0%–70%) in the LCX, and 26% \pm 19% (range, 0%–73%) in the RCA, and these values were not significantly different from one another. Six subjects (20%) presented with \geq 50% stenosis of the lumen diameter. Three subjects (10%) had mild (<30%) stenosis in the left main coronary artery.

Results of Radionuclide Studies

All subjects had normal perfusion (MIBI uptake \geq 50% of maximal myocardial MIBI uptake) at rest and during exercise, and normal perfusion was also visually confirmed by an experienced clinician. Relative MIBI uptake at rest and during exercise did not significantly differ from each other in the antero-septal region (0.65 \pm 0.04 vs. 0.64 \pm 0.03, respectively) or in the lateral region (0.58 \pm 0.04 vs. 0.57 \pm 0.05, respectively). However, the inferior myocardial region showed lower relative MIBI uptake during exercise than at rest (0.55 \pm 0.06 vs. 0.60 \pm 0.06, respectively; $P < 0.01$).

Early MIBG uptake in the antero-septal region (0.63 \pm 0.04) was higher than uptake in the lateral (0.57 \pm 0.06; $P < 0.001$) or inferior (0.58 \pm 0.06; $P < 0.001$) region. In delayed scintigraphy imaging, MIBG uptake in the antero-

septal region (0.39 \pm 0.06) did not differ from that in the lateral region (0.37 \pm 0.07) but was significantly higher than that in the inferior region (0.34 \pm 0.06; $P < 0.001$).

The average global MIBG washout rate as assessed by planar imaging was 38% \pm 9%. MIBG washout in the antero-septal region (38% \pm 10%) did not differ from that in the lateral (36% \pm 12%) or inferior (41% \pm 8%) region. However, MIBG washout in the inferior region was higher than that in the lateral region ($P < 0.05$).

Relationship Between Angiographic Findings and Regional Radionuclide Measures

We found no correlation between the severity of coronary artery stenoses in the LAD, LCX, or RCA and the uptake of MIBI in the antero-septal, lateral, or inferior myocardial regions, respectively, at rest or during exercise (Fig. 2).

The severity of LAD stenosis showed no correlation with early MIBG uptake in the antero-septal myocardial region ($r = 0.26$; $P =$ not statistically significant). On the other hand, the severity of LAD stenosis correlated directly with delayed MIBG uptake ($r = 0.43$; $P < 0.05$) and inversely with MIBG washout ($r = -0.34$; $P = 0.06$) in the antero-septal myocardial region (Fig. 2). Correspondingly, delayed MIBG uptake in the antero-septal myocardium was significantly lower in the lowest (0.34 \pm 0.05) than in the middle (0.41 \pm 0.06; $P < 0.01$) or the highest (0.43 \pm 0.05; $P < 0.001$) LAD tertile (Fig. 3A). In addition, MIBG washout in the antero-septal region was faster in the lowest LAD tertile (44% \pm 7%) than in the middle (36% \pm 10%; $P < 0.05$) or the highest LAD tertile (34% \pm 8%; $P < 0.01$) (Fig. 3B). The index of global MIBG uptake, delayed H/M, was also significantly higher in the highest LAD tertile than in the lowest LAD tertile (2.3 \pm 0.3 vs. 2.0 \pm 0.2, respectively; $P < 0.05$).

The severity of stenoses in the LCX or RCA did not correlate with initial or delayed MIBG uptake or with MIBG washout in the corresponding myocardial regions. On the other hand, delayed MIBG uptake in the lateral region was significantly lower in the lowest LCX tertile than in the middle LCX tertile (0.34 \pm 0.04 vs. 0.41 \pm 0.06; $P < 0.01$) (Fig. 3A). Early H/M, delayed H/M, and washout were not related to the severity of stenoses in the LCX or RCA.

Relationship Between Regional MIBI and MIBG Measures

Regional MIBI uptake assessed at rest or during exercise did not correlate with MIBG uptake or MIBG washout of the antero-septal or lateral myocardial region. On the other hand, MIBI uptake in the inferior region correlated directly with MIBG uptake in the corresponding region at rest ($r = 0.50$; $P < 0.01$) and during exercise ($r = 0.39$; $P < 0.05$).

DISCUSSION

The novel finding of our study was that the severity of coronary artery stenosis was associated with decreased

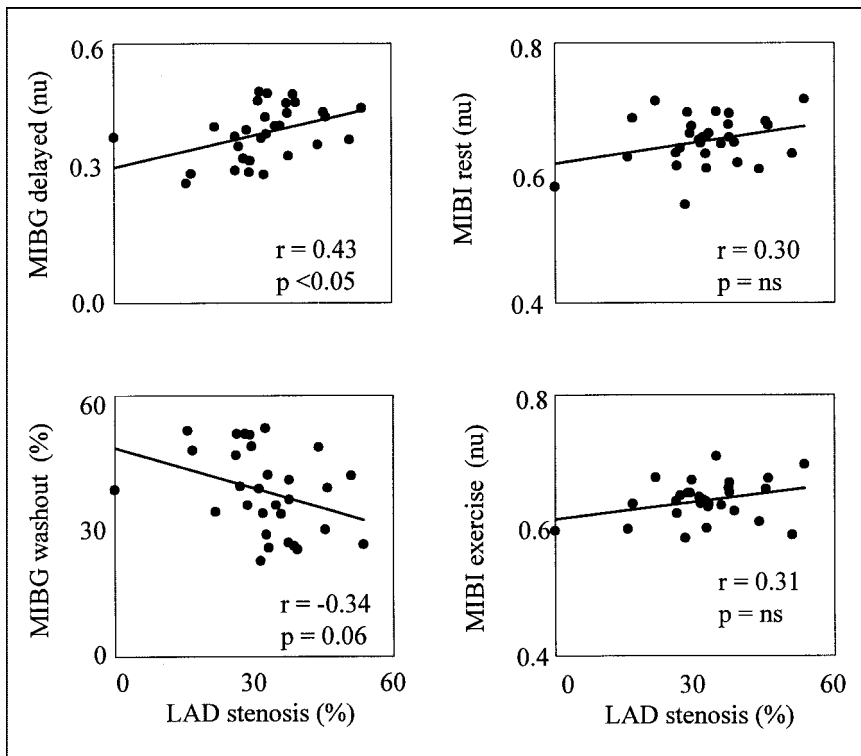


FIGURE 2. Correlation between LAD stenosis and myocardial MIBG uptake at rest and during exercise, MIBG uptake, and MIBG washout of anteroseptal myocardial region. ns = not statistically significant; nu = normalized units; rest = rest imaging.

myocardial MIBG washout in asymptomatic subjects with a very early phase of coronary artery disease, particularly in the anteroseptal myocardial region. Thus, our results imply that the function of cardiac adrenergic nerve terminals becomes affected even before hemodynamically significant stenoses develop and result in denervation.

The severity of stenoses in the LAD, and to some extent also in the LCX, was inversely related to MIBG washout and directly related to delayed MIBG uptake in the anteroseptal and lateral myocardial regions, respectively. This finding agrees well with the fact that anterolateral myocardium perfused by the LAD and LCX has the most abundant adrenergic innervation (23). Furthermore, because the subjects were asymptomatic, it seems that myocardial MIBG kinetics, reflecting cardiac adrenergic function, respond sensitively to the development of coronary artery disease. The decrease in MIBG washout that occurs during the evolution of mild coronary artery stenosis before the stenosis is severe enough to result in denervation (which is associated with increased MIBG washout) suggests biphasic changes in myocardial MIBG kinetics during ischemic progression.

In this study, early MIBG uptake did not correlate with the severity of stenosis at any respective myocardial region. Bearing in mind that early MIBG uptake represents predominantly myocardial perfusion, one would expect this finding; most stenoses were mild, and none of the subjects had symptoms suggestive of hemodynamically significant coronary artery disease. Moreover, myocardial MIBG uptake or MIBG washout was not related to perfusion of the anteroseptal or lateral myocardial regions at rest or during

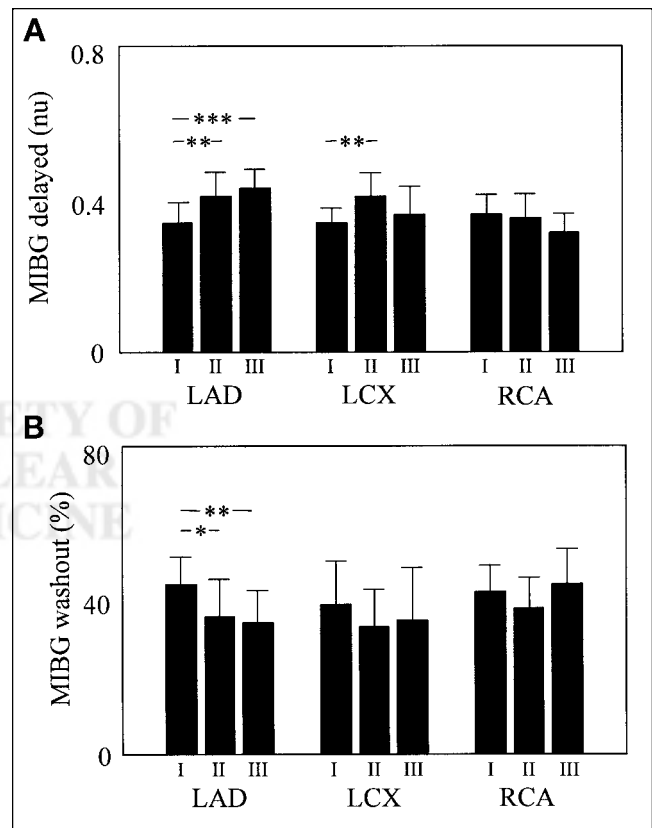


FIGURE 3. Delayed regional myocardial MIBG uptake (A) and regional myocardial MIBG washout (B) divided into tertiles according to stenoses of respective coronary artery. I = lowest tertile; II = middle tertile; III = highest tertile; nu = normalized unit. * $P < 0.05$. ** $P < 0.01$. *** $P < 0.001$.

exercise (the correlation between MIBG and MIBI uptake in the inferior region was most obviously caused by attenuation). Thus, we think that chronic ischemic damage of nerve endings does not explain our results.

Endothelial dysfunction is associated with paradoxical vasoconstriction of coronary arteries during adrenergic stimulus (24). There is also evidence that mast cells can be activated by neural stimulation (25,26) and that activated mast cells in the atherosclerotic vessel wall release a variety of vasoactive agents (27), of which histamine (28,29) and leukotrienes (30) can constrict atherosclerotic coronary segments. Accordingly, interaction between the neural and humoral systems may also contribute to abnormal vasoconstriction (31–33). It is possible that decreased cardiac adrenergic activity may protect against unopposed vasoconstriction of sclerotic coronary arteries during the development of coronary artery disease, but the mechanisms behind this modulation remain unclear.

Studies on healthy volunteers have shown that MIBG uptake of the inferior region decreases with advancing age (34,35). In these studies, MIBG uptake in the inferior region and MIBG uptake in the anterior region have been compared with each other and have not been normalized against a fixed reference region. Thus, changes in MIBG uptake with aging can result from increased anterior MIBG uptake, decreased inferior MIBG uptake, or both. On the other hand, mild, asymptomatic atherosclerotic lesions have not been previously considered an explanation for changes in MIBG kinetics. Moreover, the association between age and myocardial MIBG uptake has not been confirmed in all studies (36). Accordingly, we suggest that changes in the MIBG kinetics caused by mild atherosclerotic lesions might have been previously considered a variation of normal because no picture about the extent of atherosclerotic disease had been provided. In our study, the age range of subjects was narrow; thus, aging itself was unlikely to have had a significant confounding effect.

The overall radionuclide uptake was lowest in the inferior myocardium, most plausibly because of the attenuation of gamma radiation, a well-known limitation of SPECT imaging. On the other hand, the density of adrenergic nerve terminals is lower in the inferior myocardial region than in the anterior region, and obviously, lower MIBG uptake in the inferior region should result (35). However, attenuation has no effect on the washout analysis, because it represents the relative difference between the initial and delayed acquisitions instead of the absolute values. Thus, we assume that attenuation does not compromise comparisons of regional MIBG washout.

The decreased relative MIBI uptake in the inferior myocardial region during exercise, as compared with uptake at rest, may be caused by a smaller perfusion reserve in that region than in the antero-septal or lateral myocardial region. Another possibility is that scattered radiation from the liver or intestine enhances regional uptake during the rest study. Differences in the attenuation are not probable, because

subject positioning under the gamma camera was similar at rest and during exercise.

We assumed that the antero-septal, lateral, and inferior regions represent perfusion by the LAD, LCX, and RCA, respectively, as has previously been described (22). We admit that this is not always true, particularly when the left or right coronary artery clearly dominates myocardial perfusion or when rich collateral circulation is present. However, we found no abnormal dominance of coronary artery distribution or significant collaterals in our subjects.

CONCLUSION

The severity of coronary artery narrowing correlated inversely with cardiac adrenergic activity—as assessed by MIBG kinetics—during the early phase of coronary artery disease. This finding suggests that cardiac adrenergic function may become impaired during the early stages of coronary atherosclerosis, possibly as a protective mechanism against abnormal vasoconstriction.

REFERENCES

1. Reddy KG, Nair RN, Sheehan HM, Hodgson JM. Evidence that selective endothelial dysfunction may occur in the absence of angiographic or ultrasound atherosclerosis in patients with risk factors for atherosclerosis. *J Am Coll Cardiol*. 1994;23:833–843.
2. Zeiher AM, Drexler H, Wollschlaeger H, Just H. Modulation of coronary vasomotor tone in humans: progressive endothelial dysfunction with different early stages of coronary atherosclerosis. *Circulation*. 1991;83:391–401.
3. Vita JA, Treasure CB, Nabel EG, et al. Coronary vasomotor response to acetylcholine relates to risk factors for coronary artery disease. *Circulation*. 1990;81:491–497.
4. Schachinger V, Zeiher AM. Quantitative assessment of coronary vasoreactivity in humans in vivo: importance of baseline vasomotor tone in atherosclerosis. *Circulation*. 1995;92:2087–2094.
5. Gage JE, Hess OM, Murakami T, Ritter M, Grimm J, Krayenbuehl HP. Vasoconstriction of stenotic coronary arteries during dynamic exercise in patients with classic angina pectoris: reversibility by nitroglycerin. *Circulation*. 1986;73:865–876.
6. Zeiher AM, Drexler H, Wollschlaeger H, Saubier B, Just H. Coronary vasomotion in response to sympathetic stimulation in humans: importance of the functional integrity of the endothelium. *J Am Coll Cardiol*. 1989;14:1181–1190.
7. Dakak N, Quyyumi AA, Eisenhofer G, Goldstein DS, Cannon RO. Sympathetically mediated effects of mental stress on the cardiac microcirculation of patients with coronary artery disease. *Am J Cardiol*. 1995;76:125–130.
8. Simula S, Lakka T, Laitinen T, et al. Cardiac adrenergic denervation in patients with non-Q-wave versus Q-wave myocardial infarction. *Eur J Nucl Med*. 2000;27:816–821.
9. Stanton MS, Tuli MM, Radtke NL, et al. Regional sympathetic denervation after myocardial infarction in humans detected noninvasively using I-123-metaiodobenzylguanidine. *J Am Coll Cardiol*. 1989;14:1519–1526.
10. McGhie AI, Corbett JR, Akers MS, et al. Regional cardiac adrenergic function using I-123 meta-iodobenzylguanidine tomographic imaging after acute myocardial infarction. *Am J Cardiol*. 1991;67:236–242.
11. Dae MW, Herre JM, O'Connell JW, Botvinick EH, Newman D, Munoz L. Scintigraphic assessment of sympathetic innervation after transmural versus nontransmural myocardial infarction. *J Am Coll Cardiol*. 1991;17:1416–1423.
12. Tomoda H, Yoshioka K, Shiina Y, Tagawa R, Ide M, Suzuki Y. Regional sympathetic denervation detected by iodine 123 metaiodobenzylguanidine in non-Q-wave myocardial infarction and unstable angina. *Am Heart J*. 1994;128:452–458.
13. Hartikainen J, Mustonen J, Kuikka J, Vanninen E, Kettunen R. Cardiac sympathetic denervation in patients with coronary artery disease without previous myocardial infarction. *Am J Cardiol*. 1997;80:273–277.
14. Henderson EB, Kahn JK, Corbett JR, et al. Abnormal I-123 metaiodobenzylguanidine myocardial washout and distribution may reflect myocardial adrenergic derangement in patients with congestive cardiomyopathy. *Circulation*. 1988;78:1192–1199.

15. Kurata C, Shouda S, Mikami T, et al. Comparison of [¹²³I]metaiodobenzylguanidine kinetics with heart rate variability and plasma norepinephrine level. *J Nucl Med.* 1997;4:515–523.
16. Santos MS, Moreno AJ, Carvalho AP. Relationships between ATP depletion, membrane potential, and the release of neurotransmitters in rat nerve terminals: an in vitro study under conditions that mimic anoxia, hypoglycemia, and ischemia. *Stroke.* 1996;27:941–950.
17. Remme WJ, Kruyssen DA, Look MP, Bootsma M, de Leeuw PW. Systemic and cardiac neuroendocrine activation and severity of myocardial ischemia in humans. *J Am Coll Cardiol.* 1994;23:82–91.
18. Kline RC, Swanson DP, Wieland DM, et al. Myocardial imaging in man with I-123 meta-iodobenzylguanidine. *J Nucl Med.* 1981;22:129–132.
19. Khafagi FA, Shapiro B, Fig LM, Mallette S, Sisson JC. Labetalol reduces iodine-131 MIBG uptake by pheochromocytoma and normal tissues. *J Nucl Med.* 1989;30:481–489.
20. Syväne M, Nieminen MS, Frick MH. Accuracy and precision of quantitative arteriography in the evaluation of coronary artery disease after coronary bypass surgery: a validation study. *Int J Card Imaging.* 1994;10:243–252.
21. Reiber JHC, van der Zwet PMJ, von Land CD, et al. Quantitative coronary arteriography: equipment and technical requirements. In: Reiber JHC, Serruys PW, eds. *Advances in Quantitative Coronary Arteriography.* Dordrecht, The Netherlands: Kluwer Academic Publisher; 1993:111.
22. Kugiyama K, Yasue H, Okumura K, et al. Simultaneous multivessel coronary artery spasm demonstrated by quantitative analysis of thallium-201 single photon emission computed tomography. *Am J Cardiol.* 1987;60:1009–1014.
23. Gill JS, Hunter GJ, Gane G, Camm AJ. Heterogeneity of the human myocardial sympathetic innervation: in vivo demonstration by iodine 123-labeled meta-iodobenzylguanidine scintigraphy. *Am Heart J.* 1993;126:390–398.
24. Baumgart D, Haude M, Gorge G, et al. Augmented alpha-adrenergic constriction of atherosclerotic human coronary arteries. *Circulation.* 1999;99:2090–2097.
25. Spanos C, Pang X, Ligris K, et al. Stress-induced bladder mast cell activation: implications for interstitial cystitis. *J Urol.* 1997;157:669–672.
26. Skofitsch G, Savitt JM, Jacobowitz DM. Suggestive evidence for a functional unit between mast cells and substance P fibers in the rat diaphragm and mesentery. *Histochemistry.* 1985;82:5–8.
27. Galli SJ. New concepts about the mast cell. *N Engl J Med.* 1993;328:257–265.
28. Ginsburg R, Bristow MR, Davis K, et al. Quantitative pharmacologic responses of normal and atherosclerotic isolated human epicardial coronary arteries. *Circulation.* 1984;69:430–440.
29. Kalsner S, Richards R. Coronary arteries of cardiac patients are hyperreactive and contain stores of amines: a mechanism for coronary spasm. *Science.* 1984;223:1435–1437.
30. Allen S, Dashwood M, Morrison K, Yacoub M. Differential leukotriene constrictor responses in human atherosclerotic coronary arteries. *Circulation.* 1998;97:2406–2413.
31. Willerson JT, Golino P, Eidt J, Campbell WB, Buja LM. Specific platelet mediators and unstable coronary artery lesions: experimental evidence and potential clinical implications. *Circulation.* 1989;80:198–205.
32. Yeung AC, Vekshtein VI, Krantz DS, et al. The effect of atherosclerosis on the vasomotor response of coronary arteries to mental stress. *N Engl J Med.* 1991;325:1551–1556.
33. Laine P, Naukkarinen A, Heikkilä L, Penttilä A, Kovanen PT. Adventitial mast cells connect with sensory nerve fibers in atherosclerotic coronary arteries. *Circulation.* 2000;101:1665–1669.
34. Sakata K, Shirota M, Yoshida H, Kurata C. Physiological fluctuation of the human left ventricle sympathetic nervous system assessed by iodine-123-MIBG. *J Nucl Med.* 1998;39:1667–1671.
35. Tsuchimochi S, Tamaki N, Tadamura E, et al. Age and gender differences in normal myocardial adrenergic neuronal function evaluated by iodine-123-MIBG imaging. *J Nucl Med.* 1995;36:969–974.
36. Somsen GA, Borm JJ, Dubois EA, Schook MB, Van Der Wall EE, Van Royen EA. Cardiac ¹²³I-MIBG uptake is affected by variable uptake in reference regions: implications for interpretation in clinical studies. *Nucl Med Commun.* 1996;17:872–876.

